Upper bound of fragility from spatial fluctuations of shear modulus and boson peak in glasses

V. N. Novikov

Institute of Automation and Electrometry, Siberian Branch of the Russian Academy of Sciences, 1 Koptyug Avenue, Novosibirsk 630090, Russia

(Received 14 February 2022; accepted 1 August 2022; published 31 August 2022)

It is shown that the normalized rms fluctuation of the shear modulus on the medium-range order scale in glasses correlates with fragility: the higher fragility, the smaller the fluctuation amplitude. The latter is calculated within the heterogeneous elasticity theory using the data on the boson peak in glasses. On a smaller scale corresponding to cooperative structural relaxation, the normalized rms fluctuation of the infinite-frequency shear modulus was estimated using the data on the decoupling of viscosity and diffusion in supercooled liquids. These fluctuations are much smaller in amplitude, and, in contrast, they increase with increasing fragility. Extrapolation predicts intersection of both rms fluctuations and disappearing of the boson peak at the upper limit to fragility $\approx$180.

DOI: 10.1103/PhysRevE.106.024611

I. INTRODUCTION

Due to disordered structure, glasses have much more complex vibrational and relaxational dynamics than crystals [1]. The most noticeable feature that distinguishes the spectrum of acoustic vibrations in glasses from that in crystals is the boson peak [2–4]. It corresponds to excess acoustic vibrations with a wavelength a few times larger than the molecular size, which corresponds to the typical length of the medium-range order (MRO). It was shown that the heterogeneity of the shear modulus on the nanometer scale can explain the appearance of these excess vibrations [3,5–9]. Other models have also been proposed to describe the boson peak [10–25]. The structural disorder also leads to a complex pattern of structural relaxation in supercooled liquids [1,26]. The main feature here is the structural α relaxation. The slowing down of α relaxation with decreasing temperature leads to glass transition at a certain temperature T_g, below which the structure freezes on a laboratory time scale. One of the most important parameters characterizing glass transition is fragility m, which shows how much α-relaxation time τ_α or viscosity η changes with a change in temperature near the glass transition temperature T_g. The formal definition is $m = d\log\tau_\alpha/d(T_g/T)|_{T=Tg}$ [1,27]. Fragility changes from 18–22 for strong glass formers like silica (covalent bonding) to 160–180 for the most fragile molecular liquids and polymers [28,29]. It was found that some properties of α relaxation in supercooled liquids correlate with the elastic properties of corresponding glasses, e.g., the boson peak correlates with fragility—its amplitude is larger in strong glass formers and smaller in fragile ones [30,31] and fragility correlates with the nonergodicity parameter [32] and Poisson's ratio [31]. Note that the last correlation does not hold in complex glasses like silicates, borates, etc. [33–35], in highly fragile polymers [33], and looks different in bulk metallic glasses [34–36].

The frequency of the boson peak ν_b and the transverse sound velocity c_t of plane-wave phonons define a length

$$L_b = c_t/\nu_b \tag{1}$$

which corresponds to an acoustic wavelength of one to several nanometers. The transverse sound velocity is used in Eq. (1) because the vibrations responsible for the boson peak are of the transverse type. This is known both from the high depolarization ratio of the low-frequency Raman scattering in glasses [37–39] and computer simulation of the boson peak [40,41]. L_b is the wavelength that transverse vibrations of frequency ν_b would have in a continuous elastic medium with constant transverse sound velocity c_t. In this paper, L_b is called dynamical length because it is associated with a dynamical property.

In Refs [3,5,7,42,43], it was argued that L_b with a coefficient of the order of unity is equal to the typical length of an elastic inhomogeneity or the correlation length of spatial fluctuations of elastic constants on the scale of the MRO. The latter can be characterized by a correlation length L_c. It can be found from the static structure factor $S(q)$ based on the width ΔQ of the first diffraction peak that describes the medium-range ordering of the main structural units [44–47]:

$$L_c = 2\pi/\Delta Q. \tag{2}$$

Here ΔQ is the half width at half maximum of the diffraction peak. The respective structural units might be of various natures, in particular, basic structural units determined by the short-range order [47], rings [48], or nanovoids [49].

The two lengths, dynamical and static structure correlation lengths, are of the same order; they both are determined by the MRO scale. However, their ratio is not universal in different glasses but systematically changes with fragility. Figure 1 shows the ratio of the dynamical to static correlation length L_b/L_c for glass-forming materials with different fragility. The experimental data on c_t, ν_b, and $S(q)$ are available in Tables S1 and S2 of the Supplemental Material [50].

As shown in the inset of Fig. 1, in log-log coordinates, this correlation is a linear function. The ratio changes from about 1.8 for strong silica to about 0.5 for fragile toluene and propylene carbonate. In this paper, it is shown that this correlation can be explained by the dependence of the mean-square

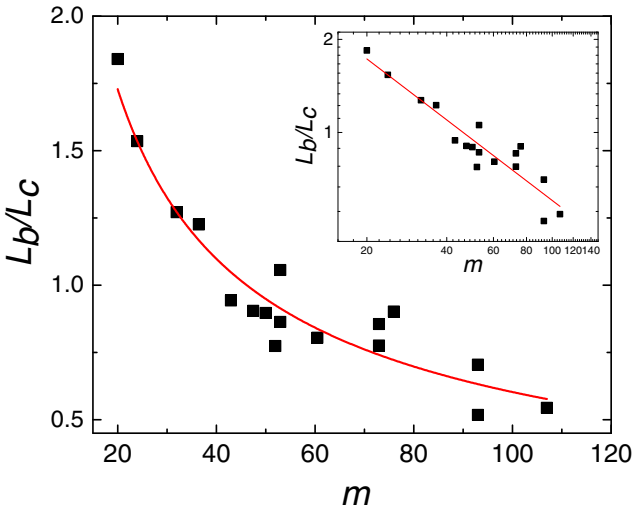

FIG. 1. Correlation of the ratio L_b/L_c with fragility. Inset: The same plot in log-log coordinates. The red solid line is a linear fit of the log-log plot which corresponds to $L_b/L_c = (13.4 \pm 2.4)/m^{0.67\pm0.05}$. In ascending order of fragility, SiO_2, GeO_2, B_2O_3, $(Li_2O)_{0.08}(B_2O_3)_{0.92}$, $Zr_{46.75}Ti_{8.25}Cu_{7.5}Ni_{10}Be_{27.5}$ (Vit4), $(Li_2O)_{0.14}(B_2O_3)_{0.86}$, $(K_2O)_{0.22}(B_2O_3)_{0.78}$, propylene glycol, glycerol, $(Na_2O)_{0.22}(B_2O_3)_{0.78}$, $(Li_2O)_{0.22}(B_2O_3)_{0.78}$, Se, salol, trisnapthylbenzene, orthoterphenyl, propylene carbonate, sorbitol, and toluene.

amplitude of the shear modulus fluctuations $\gamma_b^2 = \langle(\Delta G/G)^2\rangle$ on the nanometer scale on fragility. I found γ_b^2 for various glasses based on the heterogeneous elasticity theory using the data on the position of the boson peak and the width of the First Sharp Diffraction Peak (FSDP). As expected, γ_b^2 is larger in glasses with a strong boson peak and, respectively, with smaller fragility.

The shear modulus and its spatial fluctuations are used also in description of the α relaxation. According to one of the versions of the elastic theory of relaxation in supercooled liquids, the activation energy of the α-relaxation time τ_α is determined by the instantaneous shear modulus $G_\infty(T)$ [51,52]. The spatial fluctuations of G_∞ lead to decoupling in the temperature dependence of the diffusion and viscosity [53–57]. This is an alternative way to estimate shear modulus fluctuations. It predicts much smaller values of the elastic fluctuations than that from the boson peak. Moreover, the respective mean-square fluctuation increases with increasing fragility. Extrapolation of both correlations to higher values of fragility shows that they intersect at $m \approx 180$, which is close to the upper bound of fragility in supercooled liquids [28,58–61]. A spatial landscape of the shear modulus in glasses corresponding to these results is proposed.

II. THEORY AND RESULTS

To find the relationship between the dynamical length L_b and the static length characterizing structure heterogeneity L_c, perturbation theory for fluctuations of elastic constants of glass in combination with the Ioffe-Regel (IR) criterion of localization [62–66] is used here. It is known that the IR criterion is fulfilled for transverse vibrations in glasses at the frequency of the boson peak [63]. The IR criterion for transverse vibrations is

$$\Gamma_t(\omega) = \omega/\pi, \tag{3}$$

where $\Gamma_t(\omega)$ is the full width at half maximum of the vibrational line with the frequency ω [63–66]. In terms of the vibration lifetime, this criterion is $\tau_t^{-1}(\omega) = \omega/2\pi$. Equation (3) connects the boson peak frequency, and hence the dynamic length L_b, with the parameters of the elastic heterogeneity that determine the value of Γ_t. This approach has already been used in Refs. [67,68], but in the approximation used the medium had only one modulus of elasticity and, respectively, one sound velocity.

The vibrational properties are described by the Green function:

$$G_\alpha(\boldsymbol{k}, \omega) = \frac{\omega_{k\alpha}}{\omega^2 - \omega_{k\alpha}^2 - \omega_{k\alpha}\Sigma_\alpha(\boldsymbol{k}, \omega)}, \tag{4}$$

where α corresponds to the transverse, t, or longitudinal, l, vibrational mode, and $\Sigma_\alpha(\boldsymbol{k}, \omega)$ is the respective self-energy function. Phonon lifetime is determined by the imaginary part of the self-energy function. If $\Sigma_\alpha(k, \omega) = \Sigma_{1\alpha}(k, \omega) + i\Sigma_{2\alpha}(k, \omega)$ then

$$\tau_\alpha^{-1}(\omega) = \Sigma_{2\alpha}(\omega/c_\alpha, \omega), \tag{5}$$

where c_t and c_l are transverse and longitudinal sound velocities, respectively. To estimate the self-energy function, the Hamiltonian of elastic waves for an isotropic solid in continuum approximation is used:

$$H = \int d^3r \left[\frac{\pi^2}{2\rho} + G\left(s_{ij}^2 - \frac{1}{3}s_{ii}^2\right) + \frac{K}{2}s_{ii}^2\right], \tag{6}$$

where π and ρ are the momentum and mass density,

$$s_{ij} = \frac{1}{2}\left(\frac{\partial u_i}{\partial r_j} + \frac{\partial u_j}{\partial r_i}\right) \tag{7}$$

is the strain tensor, $\boldsymbol{u}(\boldsymbol{r}, t)$ is the displacement from equilibrium,

$$u_j(\boldsymbol{r}) = \sqrt{\frac{\hbar}{\varrho V}} \sum_{\boldsymbol{k},\alpha} \frac{A_{k\alpha} e_{k\alpha,j}}{\sqrt{\omega_{k\alpha}}} e^{i\mathbf{kr}}, \tag{8}$$

where $A_{\boldsymbol{k}\alpha} = (a_{\boldsymbol{k}\alpha} + a_{-\boldsymbol{k}\alpha}^+)/\sqrt{2}$, $a_{\boldsymbol{k}\alpha}$ and $a_{\boldsymbol{k}\alpha}^+$ are phonon annihilation and creation operators, $\boldsymbol{e}_{\boldsymbol{k}\alpha}$ is the polarization vector of the phonon with momentum $\boldsymbol{k}$, and the index α describes three acoustical modes. $G(\boldsymbol{r})$ and $K(\boldsymbol{r})$ are the spatially fluctuating shear and bulk moduli, respectively, and $G(\boldsymbol{r}) = \langle G(\boldsymbol{r})\rangle + \delta G(\boldsymbol{r})$, $G(\boldsymbol{r}) = \langle K(\boldsymbol{r})\rangle + \delta K(\boldsymbol{r})$. In support of the continuum approximation of elasticity in the model used, it can be noted that the ratio of the frequency of the boson peak to the Debye frequency is, for example, about 10 in silica and 8 in glycerol. This is far enough from the end of the acoustic spectrum that the continuum approximation should be expected to work quite well. It is also known that the spectral shape of the boson peak is practically universal and does not depend on the microscopic features of the glass structure.

The perturbation term in the Hamiltonian is

$$\delta H = \int d^3r \left\{ \delta G(\boldsymbol{r}) \left(s_{ij}^2(\boldsymbol{r}) - \frac{1}{3} s_{ii}^2(\boldsymbol{r}) \right) + \frac{1}{2} \delta K(\boldsymbol{r}) s_{ii}^2(\boldsymbol{r}) \right\}. \tag{9}$$

The perturbation term expressed in terms of phonons has the form

$$\delta H = \frac{1}{2} \sum_{\boldsymbol{k},\boldsymbol{k}_1,\alpha,\alpha'} V_{\alpha\alpha'}(\boldsymbol{k},\boldsymbol{k}_1) A_{\boldsymbol{k}\alpha} A_{\boldsymbol{k}_1\alpha'}, \tag{10}$$

where

$$\begin{aligned} &V_{\alpha\alpha'}(\boldsymbol{k},\boldsymbol{k}_1) \\ &= \frac{\hbar}{V\rho(\omega_{\boldsymbol{k}\alpha}\omega_{\boldsymbol{k}_1\alpha'})^{1/2}} \Big\{ \Big[(\boldsymbol{k}\boldsymbol{k}_1)\big(\boldsymbol{e}_{\boldsymbol{k}\alpha}\boldsymbol{e}_{\boldsymbol{k}_1\alpha'}\big) + \big(\boldsymbol{k}\boldsymbol{e}_{\boldsymbol{k}_1\alpha'}\big)(\boldsymbol{k}_1\boldsymbol{e}_{\boldsymbol{k}\alpha}) \\ &\quad - \frac{2}{3}(\boldsymbol{k}\boldsymbol{e}_{\boldsymbol{k}\alpha})(\boldsymbol{k}_1\boldsymbol{e}_{\boldsymbol{k}_1\alpha'}) \Big] \\ &\quad \times (\delta G)_{\boldsymbol{k}+\boldsymbol{k}_1} + (\boldsymbol{k}\boldsymbol{e}_{\boldsymbol{k}\alpha})\big(\boldsymbol{k}_1\boldsymbol{e}_{\boldsymbol{k}_1\alpha'}\big)(\delta K)_{\boldsymbol{k}+\boldsymbol{k}_1} \Big\}. \end{aligned} \tag{11}$$

Here

$$(\delta G)_{\boldsymbol{k}} = \int d^3r e^{i\mathbf{k}\mathbf{r}} \delta G(r) \tag{12}$$

and, respectively, for $(\delta K)_{\boldsymbol{k}}$. The spatial correlation function of the fluctuations is defined as follows:

$$F(r) = \langle \delta G(\boldsymbol{R}) \delta G(\boldsymbol{r}+\boldsymbol{R}) \rangle / \langle G \rangle^2 = \gamma_b^2 e^{-\varkappa r}. \tag{13}$$

The Fourier transform of $F(r)$ is

$$F(k) = \int d^3r e^{ikr} F(r) = \frac{8\pi\varkappa\gamma_b^2}{(\varkappa^2 + k^2)^2}, \tag{14}$$

where $\varkappa^{-1}$ is the correlation radius and γ_b^2 is the mean-square fluctuation of the shear modulus on the scale relevant to the boson peak [Eq. (13)], normalized by the mean value of G:

$$\gamma_b^2 = \frac{\langle (\delta G)^2 \rangle}{\langle G \rangle^2}. \tag{15}$$

In the second-order approximation, the self-energy function is equal to

$$\begin{aligned} &\Sigma_\alpha(\boldsymbol{k},\omega) \\ &= \int \frac{d^3k_1}{(2\pi)^3} \sum_{\alpha'} \langle V_{\alpha\alpha'}(-\boldsymbol{k},\boldsymbol{k}_1) G_{0\alpha'}(\boldsymbol{k}_1,\omega) V_{\alpha'\alpha}(-\boldsymbol{k}_1,\boldsymbol{k}) \rangle \\ &= \frac{2\hbar^2 v_t^4 \gamma_b^2 \varkappa}{\pi} \int \frac{k_1^2 d\, k_1 \sin\theta d\theta}{\left(\varkappa^2 + k_1^2 + k^2 - 2k\, k_1 \cos\theta\right)^3} \\ &\quad \times \sum_{\alpha'} \frac{G_{0\alpha'}(\boldsymbol{k}_1,\,\omega) \overline{Q_{\alpha\alpha'}^2}(\boldsymbol{k},\boldsymbol{k}_1)}{\omega_{\boldsymbol{k}\alpha}\omega_{\boldsymbol{k}_1\alpha'}}, \end{aligned} \tag{16}$$

where

$$\begin{aligned} Q_{\alpha\alpha'}(\boldsymbol{k},\boldsymbol{k}_1) = {} & (\boldsymbol{k}\boldsymbol{k}_1)\big(\boldsymbol{e}_{\boldsymbol{k}\alpha}\boldsymbol{e}_{\boldsymbol{k}_1\alpha'}\big) + \big(\boldsymbol{k}\boldsymbol{e}_{\boldsymbol{k}_1\alpha'}\big)(\boldsymbol{k}_1\boldsymbol{e}_{\boldsymbol{k}\alpha}) \\ & - \tfrac{2}{3}(\boldsymbol{k}\boldsymbol{e}_{\boldsymbol{k}\alpha})\big(\boldsymbol{k}_1\boldsymbol{e}_{\boldsymbol{k}_1\alpha'}\big) \end{aligned} \tag{17}$$

is symmetrical with respect to $\boldsymbol{k}$, $\boldsymbol{k}_1$, as well as α, α'; θ is the angle between vectors $\boldsymbol{k}$ and $\boldsymbol{k}_1$.

Note that Eq. (15) is a complete expression for Σ_t only, and in the case of Σ_l there are also terms with $\langle \delta K(\boldsymbol{r}) \delta K(\boldsymbol{r}+\boldsymbol{R}) \rangle$ and $\langle \delta G(\boldsymbol{r}) \delta K(\boldsymbol{r}+\boldsymbol{R}) \rangle$ on the right-hand side (see Sec. II of the Supplemental Material [50]). They are absent in Σ_t because of polarization symmetry. In addition, density fluctuations at this nanometer scale were neglected, since their contribution is much less than the contribution of the shear modulus, i.e., in silica $\langle (\delta\rho/\rho)^2 \rangle \approx 0.01$ [43] in comparison with $\gamma_b^2 \approx 0.36$ of this paper (see below). Since G and ρ enter the problem in the combination $G/\rho = c_t^2$, considering $\langle (\delta c_t/c_t)^2 \rangle$ as a small parameter instead of $\langle (\delta G/G)^2 \rangle$ allows one to take into account density fluctuations more accurately. Neglecting the latter gives $\langle (\delta G/G)^2 \rangle = 4\langle (\delta c_t/c_t)^2 \rangle$.

The overbar in $\overline{Q_{\alpha\alpha'}^2}(\boldsymbol{k},\boldsymbol{k}_1)$ in Eq. (16) means averaging over phonon polarization directions, which is done using relations

$$\overline{e_{\boldsymbol{k}l,i} e_{\boldsymbol{k}l,j}} = \frac{k_i k_j}{k^2} \tag{18}$$

for longitudinal phonons and

$$\overline{e_{\boldsymbol{k}t,i} e_{\boldsymbol{k}t,j}} = \frac{1}{2}\left(\delta_{ij} - \frac{k_i k_j}{k^2} \right) \tag{19}$$

for transverse phonons. Taking into account these relations, the functions $\overline{Q_{\alpha\alpha'}^2}(\boldsymbol{k},\boldsymbol{k}_1)$ are equal to

$$\overline{Q_{ll}(\boldsymbol{k},\boldsymbol{k}_1)^2} = 4k^2k_1^2\left(x^4 - \frac{2}{3}x^2 + \frac{1}{9} \right), \tag{20}$$

$$\overline{Q_{tt}(\boldsymbol{k},\boldsymbol{k}_1)^2} = k^2k_1^2\left(x^4 - \frac{3}{4}x^2 + \frac{1}{4} \right), \tag{21}$$

$$\overline{Q_{lt}(\boldsymbol{k},\boldsymbol{k}_1)^2} = \overline{Q_{tl}(\boldsymbol{k},\boldsymbol{k}_1)^2} = 2k^2k_1^2x^2(1-x^2), \tag{22}$$

where $x = \boldsymbol{k}\boldsymbol{k}_1/kk_1 = cos\theta$. As a result,

$$\begin{aligned} \Sigma_t(k,\omega) = {} & \frac{4\gamma_b^2\varkappa c_t^3 k}{\pi} \int_0^{k_D} k_1^4 dk_1 \left[\frac{Z_2(k,k_1) - Z_4(k,k_1)}{\omega^2 - v_l^2k_1^2 + i0} \right. \\ & \left. + \frac{Z_4(k,k_1) - \frac{3}{4}Z_2(k,k_1) + \frac{1}{4}Z_0(k,k_1)}{\omega^2 - v_t^2k_1^2 + i0} \right] \end{aligned} \tag{23}$$

where functions $Z_n(k,k_1)$ are defined as

$$Z_n(k,k_1) = \int_{-1}^{1} \frac{x^n dx}{\left(\varkappa^2 + k_1^2 + k^2 - 2kk_1x\right)^2}. \tag{24}$$

These integrals are estimated in analytical form in Sec. II of the Supplemental Material [50]. The imaginary part of $\Sigma_t(k,\omega)$ is equal to

$$\begin{aligned} \Sigma_{2t}(k,\omega) = {} & \frac{2\gamma_b^2\varkappa k\omega^3}{c_t^2} \left[\frac{c_t^5}{c_l^5}(Z_2(k,\omega/v_l) - Z_4(k,\omega/v_l)) \right. \\ & \left. + Z_4(k,\omega/v_t) - \frac{3}{4}Z_2(k,\omega/v_t) + \frac{1}{4}Z_0(k,\omega/v_t) \right]. \end{aligned} \tag{25}$$

Finally, using the IR criterion (3) and Eq. (5) for $\tau_t^{-1}(\omega)$, one can obtain the expression for the mean-square shear modulus fluctuation responsible for the boson peak:

$$\gamma_b^2 = \frac{\varkappa^3 R_b^3}{4\pi f}, \tag{26}$$

where $R_b = L_b/2\pi$ and f is a dimensionless function of $1/\varkappa R_b$ and c_t/c_l:

$$f = \frac{c_t^5 \varkappa^4}{c_l^5}\left[Z_2\left(\frac{1}{R_b}, \frac{1}{R_b}\frac{c_t}{c_l}\right) - Z_4\left(\frac{1}{R_b}, \frac{1}{R_b}\frac{c_t}{c_l}\right)\right] + Z_4\left(\frac{1}{R_b}, \frac{1}{R_b}\right) - \frac{3}{4}Z_2\left(\frac{1}{R_b}, \frac{1}{R_b}\right) + \frac{1}{4}Z_0\left(\frac{1}{R_b}, \frac{1}{R_b}\right). \tag{27}$$

The parameter γ_b^2 can be estimated using experimental data on the boson peak frequency, sound velocities, and assuming the MRO radius $R_c = 1/\varkappa$ is determined by the structure and thus can be taken from the diffraction data, $2R_c = L_c$, as it was suggested earlier in Ref. [43]. The estimated values of γ_b^2 are in the interval 0.36–0.05 for various glasses (see Table S2 of the Supplemental Material [50]). Interestingly, there is a correlation between fluctuations and fragility: γ_b^2 decreases with increasing fragility (Fig. 2). In log-log coordinates the dependence is a linear function (Fig. 2, inset) with a slope of about -1. The fit of the $\gamma_b^2(m)$ dependence by a power law gives $\gamma_b^2(m) \approx (6.1 \pm 1.3)/m^{0.97\pm0.06}$. Fixing the exponent in the denominator at 1 gives in a good approximation

$$\gamma_b^2(m) = \frac{6.7 \pm 0.2}{m}. \tag{28}$$

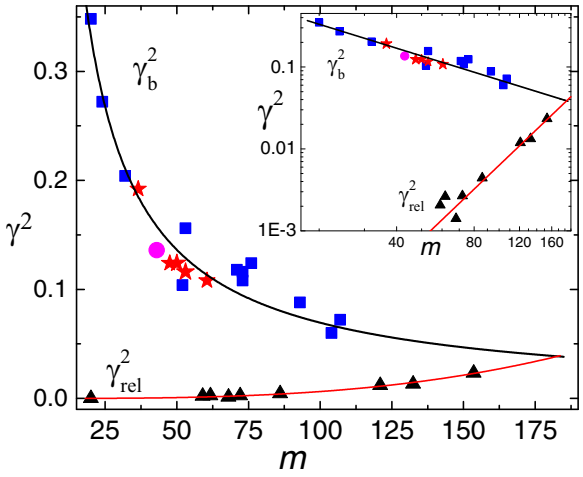

FIG. 2. Correlation of the normalized mean-square fluctuation of the shear modulus with fragility: γ_b^2, found from the boson peak; γ_{rel}^2, found from the decoupling of viscosity and diffusion in supercooled liquids. Inset: The same data in log-log scale. Blue squares: SiO_2, GeO_2, B_2O_3, propylene glycol, glycerol, Se, salol, trisnapthylbenzene (TNB), orthoterphenyl (OTP), sorbitol, propylene carbonate, and toluene. Red stars: Borate glasses $(Li_2O)_{0.08}(B_2O_3)_{0.92}$, $(Li_2O)_{0.14}(B_2O_3)_{0.86}$, $(K_2O)_{0.22}(B_2O_3)_{0.78}$ $(Na_2O)_{0.22}(B_2O_3)_{0.78}$, and $(Li_2O)_{0.22}(B_2O_3)_{0.78}$. Magenta circle: Metallic glass $Zr_{46.75}Ti_{8.25}Cu_{7.5}Ni_{10}Be_{27.5}$ (Vit4). Black triangles: Silica, polyoxybutylene, polyisoprene, TNB, polypropylene glycol, OTP, atactic polypropylene, polystyrene, and polycarbonate. Within each subgroup, materials are listed in ascending order of fragility. Solid lines are fits as described in the text.

Another way to estimate the mean-square fluctuation of the shear modulus is given by the elastic theory of relaxation in supercooled liquids in combination with data on the decoupling between viscosity and diffusion. According to one of the versions of the theory, the structural relaxation time τ_α is expressed via the instantaneous shear modulus G_∞ as

$$\tau_\alpha(T) = \tau_0 \exp\frac{G_\infty(T)V_0}{T}, \tag{29}$$

where V_0 is a temperature independent parameter of the order of molecular volume [51,52] and Boltzmann constant k_B is set equal to 1. Alternatively, $\tau_\alpha(T) = \tau_0 \exp(A/\langle u^2\rangle)$, where A is a constant, and $\langle u^2\rangle$ is particle mean-square displacement [52]. The quantity $T/\langle u^2\rangle$ can be interpreted as a local measure of material "stiffness" when $\langle u^2\rangle$ is considered on the plateau of the initial, picosecond stages of its time dependence. It is assumed here that the expression can be applied locally, in independently relaxing domains like the cooperatively rearranged regions of Adam and Gibbs [69], at least in terms of some effective local shear modulus that describes local rigidity when escaping the cage. In more detail the local rigidity and its relation to the macroscopic shear modulus are discussed in Refs. [70–74]. The respective local diffusion coefficient $D(T) \propto \tau_\alpha^{-1}(T)$. It is well known that there is a decoupling between relaxation time (or viscosity) and diffusion in supercooled liquids, which increases with decreasing temperature [53–57]. The experimental data show that the temperature dependence of decoupling is well described by a fractional Stokes-Einstein law [55,56]:

$$\bar{D}(T)\bar{\tau}_\alpha(T) \propto [\bar{\tau}_\alpha(T)]^\varepsilon \tag{30}$$

with the exponent $\varepsilon < 1$. In Eq. (30), $\bar{D}$ and $\bar{\tau}_\alpha$ are experimental values of the diffusion and relaxation time that correspond to volume-averaged local values. The dependence of the exponent ε on fragility for a number of glass-forming materials was found in Ref. [57]. It was shown that ε increases with fragility, from about zero for silica, to ~0.3 for fragile molecular liquids, and up to 0.5–0.6 for very fragile polymers [57].

Let us suppose that the distribution of the activation energy $E = G_\infty V_0$ is flat between $E = E_0$ and $(1-\varepsilon)E_0$. Outside this interval, the distribution function is zero. The average value $\langle E\rangle = \langle G\rangle V_0 = E_0(1-\varepsilon/2)$. Then

$$\bar{\tau}_\alpha(T) = \tau_0\left(\frac{T}{\varepsilon E_0}\right)\left(1 - e^{-\frac{\varepsilon E_0}{T}}\right)e^{\frac{E_0}{T}}, \tag{31}$$

$$\bar{D}(T) = D_0\left(\frac{T}{\varepsilon E_0}\right)\left(1 - e^{-\frac{\varepsilon E_0}{T}}\right)e^{-\frac{E_0}{T}+\frac{\varepsilon E_0}{T}}. \tag{32}$$

Note that, at the glass transition temperature, $E_0/T_g \sim \ln\frac{\bar{\tau}_\alpha(T_g)}{\tau_0} \approx 39$. Assuming that $\exp(-\varepsilon E_0/T) \ll 1$ holds close to T_g, with accuracy up to logarithmic terms in T in the exponent we have $\bar{D}\bar{\tau}_\alpha \propto \exp(\varepsilon E_0/T) \propto \bar{\tau}_\alpha^\varepsilon$ in accordance with the fractional Stokes-Einstein law (30). With this distribution

of activation energies, $\langle E^2\rangle = E_0^2(1-\varepsilon+\varepsilon^2/3)$, so

$$\gamma_{\rm rel} = \frac{\sqrt{\langle(\Delta E)^2\rangle}}{\langle E\rangle} = \frac{\sqrt{\langle(\Delta G_\infty)^2\rangle}}{\langle G_\infty\rangle} = \frac{\varepsilon}{2\sqrt{3}} + O(\varepsilon^2). \quad (33)$$

As expected, a higher decoupling corresponds to a higher mean-square fluctuation of the instantaneous shear modulus. The correlation of the decoupling parameter ε with fragility is quantified in Ref. [57] where both ε and fragility are given for a number of materials (see Table S3 in the Supplemental Material [50]). These data are used to plot $\gamma_{\rm rel}^2$ as a function of fragility in Fig. 2. The $\gamma_{\rm rel}^2$ values are much less than those determined by the boson peak, γ_b^2 (e.g., 0.0016 from decoupling compared to 0.12 from the boson peak for trisnapthylbenzene and 0.0044 vs 0.10 for orthoterphenyl). Moreover, the decoupling data predict an increase in $\gamma_{\rm rel}^2$ with fragility, while an estimate based on the boson peak predicts a decrease in γ_b^2 with increasing fragility. The fit of the $\gamma_{\rm rel}^2(m)$ dependence by a power law gives $\gamma_{\rm rel}^2(m) = (1.04\pm0.91)10^{-8}/m^{2.9\pm0.2}$. The exponent in this dependence on m practically does not differ from 3. If one fixes it at 3, then

$$\gamma_{\rm rel}^2(m) = \frac{(0.63\pm0.16)10^{-8}}{m^3}. \quad (34)$$

In log-log scale, both $\gamma_b^2(m)$ and $\gamma_{\rm rel}^2(m)$ correlations appear to be linear functions (Fig. 2, inset). Extrapolating both linear functions to higher fragility one can see that they eventually intersect at $m \approx 185\pm15$, where $\gamma_{\rm rel}^2 \approx \gamma_b^2 \approx 0.04$.

III. DISCUSSION

The following picture may describe two different types of $\gamma(m)$ behavior. γ_b^2 corresponds to fluctuations of the shear modulus on the MRO scale, and $\gamma_{\rm rel}^2$ corresponds to fluctuations of smaller scale, related to escape from the cage. The results show that the low-fragility glass formers have lower amplitude of the normalized shear modulus fluctuations on short scales. Smaller short-range fluctuations presumably correspond to a higher short-range order. This is what one would expect from covalently bonded materials like silica, which have a strong bond directionality that determines the short-range order. However, in such glasses, on a larger MRO scale, a sharper and more abrupt fluctuation of the shear modulus occurs. In fragile glass formers with van der Waals molecular interactions, short-range fluctuations are larger, and the gradual accumulation of disorder leads to a smother loss of correlations and a lower amplitude of shear modulus fluctuations on the MRO scale. As seen in Fig. 1, the ratio L_b/L_c reaches $\approx$2 for the strongest glass formers, such as silica. This means that in such materials the transverse vibration with the frequency ν_b has a wavelength $\lambda = L_b \sim 2L_c$, i.e., half the wavelength is equal to the diameter of the MRO region. This corresponds to the lowest-frequency vibration localized in a region of this size, if it is separated as an independent cluster. This situation is similar to the early ideas about the boson peak as vibrations localized on clusters with a medium-range order size [5,6]. In materials with higher fragilities, the vibrations with frequency ν_b have a wavelength comparable to (intermediate fragility materials) or shorter (high fragility materials) than L_c, for example, for glycerol $\lambda = L_b \sim L_c$ and for propylene carbonate and toluene $\lambda \approx 0.5L_c$.

In materials with sufficiently high fragility, the difference between the amplitude of the shear modulus fluctuations on the scales of the medium- and short-range orders disappears (Fig. 2). As seen from Fig. 2, this occurs when fragility reaches values in the range of 185 ± 15. This value is close to the upper limit to fragility $m_{\rm max} \approx 170$–190 predicted in Refs. [58–60]. In Ref. [58] fragility was expressed in terms of the thermodynamic parameters of the system, which are important for the glass transition. In particular, it was concluded that fragility of the glass formers has an upper limit of $m_{\rm max} \approx$ 170–190. In Ref. [59], the enthalpy relaxation measurements during cooling and heating across the glass transition were used to determine $m_{\rm max}$. The extrapolation of the relaxation enthalpy to zero predicted the upper limit of fragility in the interval $\approx$170–180. The value $m_{\rm max} \approx$ 175–180 follows also from the ratio of the relaxation widths of structural α and β relaxations [59,60], and from the ratio of the configurational heat capacity and the total heat capacity jump at glass transition [59,61]. In terms of the present paper, the limiting fragility corresponds to the situation when the relative amplitude of the medium-range fluctuations of the shear modulus, γ_b^2, becomes equal to the amplitude of the normalized short-range fluctuations of α-relaxation activation energy, or instantaneous shear modulus, $\gamma_{\rm rel}^2$, in the supercooled liquid state near T_g. In different words, in materials with $m = m_{\rm max}$, the normalized amplitude of elasticity fluctuations between uncorrelated domains on the MRO scale is of the same order as that of the activation energy of α relaxation (determined by the instantaneous shear modulus) inside these domains. The latter is much smaller than the former in materials with fragilities $m < m_{\rm max}$, by a factor $\approx(m/m_{\rm max})^4$. Respectively, according to Eqs. (28) and (34), the product of $\gamma_{\rm rel}$ by γ_b^3 is a universal constant for various glasses, $\gamma_{\rm rel}\gamma_b^3 = (1.5\pm0.1)\times10^{-3}$.

One of the consequences of this picture is that the boson peak should disappear when fragility reaches its upper limit value. The boson peak can be characterized by its normalized amplitude $A_{\rm BP}$, defined as

$$A_{\rm BP} = \left.\frac{g(\omega)}{g_D(\omega)}\right|_{\rm max}, \quad (35)$$

where $g(\omega)$ is the density of vibrational states, $g_D(\omega) = 3\omega^2/\omega_D^3$ is the Debye density of vibrational states, $\omega_D = c_D(6\pi^2 n)^{1/2}$ is the Debye frequency, and Debye velocity c_D is defined by the equation $3/c_D^3 = 2/c_t^3 + 1/c_l^3$. The absence of the boson peak corresponds to $A_{\rm BP} = 1$. In Fig. 3 the correlation of $A_{\rm BP}$ with fragility for various glasses is shown. To find $A_{\rm BP}$, the inelastic neutron scattering data from literature are used. $A_{\rm BP}$ is maximum for silica glass ($A_{\rm BP} \approx 6$) and it is only 1.6–1.8 for glass formers with fragility of about 100. In log-log coordinates, the correlation $A_{\rm BP}$ with fragility is well represented by the linear function (Fig. 3). The solid line in Fig. 3 corresponds to the power law $A_{\rm BP} \propto m^{-0.8}$, which is a recent prediction of the heterogeneous elasticity theory [75]. It is in reasonable agreement with the experimental data. Only one point, corresponding to B_2O_3 (second point from the left), noticeably deviates from the linear dependence of the correlation in log-log coordinates. This point is at small

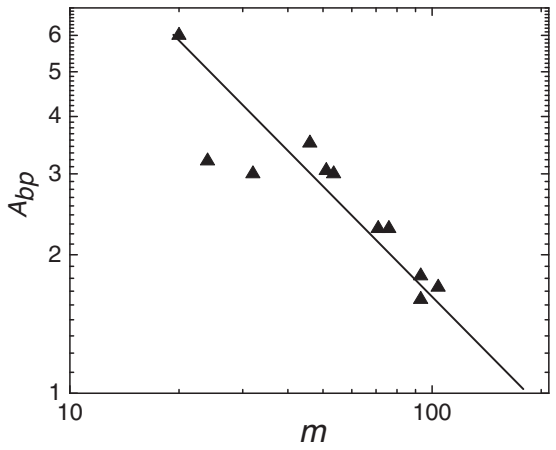

FIG. 3. Amplitude of the boson peak A_{BP} from neutron scattering data [Eq. (35)] vs fragility in log-log coordinates. In order of increasing fragility, SiO_2, GeO_2, B_2O_3, polyisobutylene (PIB), propylene glycol, glycerol, Se, orthoterphenyl, $Ca_{0.4}K_{0.6}(NO_3)_{1.4}$ (CKN), sorbitol, and propylene carbonate. The solid line corresponds to $A_{BP} \propto m^{-0.8}$. Literature data and respective references for A_{BP} and fragility are in Table S4 of Supplemental Material [50].

values of fragility. The rest of the points quite clearly show a linear correlation. Extrapolation of A_{BP} (m) dependence to higher values of fragility shows that the boson peak should disappear from the vibrational spectrum at $m \approx 170 \div 200$, when $A_{BP} \to 1$. This experimental observation supports the above prediction about the disappearance of the boson peak when fragility reaches its upper limit.

Let us summarize the main assumptions and limitations that are essential for the results obtained. Continuum approximation and perturbation theory with respect to γ_b^2 were already discussed in Secs. I and II. The parameter γ_b^2 was obtained in the range $\leqslant 1/10$ for fragile glass formers to $\approx 1/3$ for most strong glass formers, which supports the applicability of perturbation theory. Another assumption concerns the description of decoupling of viscosity and diffusion upon cooling supercooled liquids. It was assumed, in agreement with Refs. [55,56], that this effect, close to T_g, is caused by the spatial heterogeneity of dynamics, which is regulated by the local activation barriers. For the latter, the elastic theory of the relaxation in supercooled liquids was applied, limited by the region close to T_g. Another important assumption, used for finding the upper limit of fragility, is that the linear dependence of log γ_b^2 on log m observed in the range of fragilities $\approx$20–105 can be extrapolated to higher values of fragility. The same assumption was used for log γ_{rel}^2 vs log m linear dependence. Note that the same assumption was applied to find the upper bound of fragility in Refs. [58–61]. This is the same as assuming that the mechanisms leading to the linear behavior of correlation stay the same in materials which have fragilities in the range between the last experimental point in Fig. 2 and m_{max}. The accuracy of the predicted value of m_{max} is limited by the number of materials for which all the necessary data are available in literature. One needs to know the position of the boson peak, its amplitude relative to the Debye density of states, transverse and longitudinal sound velocity, static structure factor, and fragility. For structural relaxation data, one needs to know the exponent of the fractional Stokes-Einstein law and fragility. The lack of data limits the number and variety of materials on the correlation plots (Figs. 1–3). The list of studied materials includes some covalently bonded, hydrogen bonded, molecular, polymeric glasses; one bulk metallic glass; as well as some complex borate glasses. However, the limited number and variety of studied materials do not yet allow us to conclude how universal the correlations found are. Further investigations are needed to clarify this question.

IV. CONCLUSIONS

In conclusion, the nanometer-scale dynamical length L_b defined by the boson peak frequency and transverse sound velocity was compared with the static medium-range correlation length of the structure L_c. Their ratio L_b/L_c correlates with fragility of glass formers, being higher in strong glass formers and lower for fragile ones. The estimation of the dynamical length using perturbation theory based on the fluctuations of the shear modulus and the IR criterion for transverse vibrations showed that the L_b/L_c ratio in glasses is determined by two factors—the normalized strength of shear modulus fluctuations γ_b^2 and the ratio of the transverse and longitudinal sound velocities c_t/c_l (or shear and bulk moduli). This relationship allows one to express γ_b^2 on the length scale of the MRO in terms of L_b/L_c and c_t/c_l. The parameter γ_b^2 varies in the range 0.06–0.35 for 18 different glasses with fragilities in the range $\approx$20–110, and has a power-law correlation with fragility, approximately, $\gamma_b^2 \propto m^{-1}$. This is consistent with the well-known observation that stronger glasses have a higher boson peak amplitude [30,33], since the latter should increase with the parameter γ_b^2.

The mean-square shear modulus fluctuations can be estimated also based on the structure relaxation properties of glass formers. To this end, the elastic theory of relaxation in supercooled liquids [51,52] is used here to describe the decoupling between viscosity and diffusion in terms of shear modulus spatial fluctuations. It is assumed that the decoupling is caused by the spatial heterogeneity of dynamics [55,56]. It is found that the respective normalized mean-square fluctuation γ_{rel}^2 is much smaller than γ_b^2 and increases with increasing fragility approximately as $\gamma_{rel}^2 \propto m^3$. Extrapolation of the dependencies $\gamma_b^2(m)$ and $\gamma_{rel}^2(m)$ to high fragilities shows that they intersect at about $m \approx 185 \pm 15$, i.e., close to the upper bound of fragility m_{max} found by other methods [28,58–61]. These results are explained in a model in which the spatial heterogeneity of the shear modulus on the scale of MRO, characterized by γ_b^2, determines the amplitude and, to some extent, the position of the boson peak. At a shorter length, within the correlated medium-range domains, fluctuations of the barriers for structural relaxation, characterized by γ_{rel}^2 and determined by the local instantaneous shear modulus, are significantly smaller than between domains. They determine the decoupling of viscosity and diffusion in this model and increase with fragility. In materials with $m \sim m_{max}$, dispersion of the shear modulus between the different medium-range correlated regions becomes close to that for the shorter-range fluctuations within the regions. In this sense, the medium-range heterogeneity is not well defined in such glasses and

there should be no boson peak in the vibrational spectrum. This scenario is confirmed by the analysis of the experimental data on the boson peak. However, the limited number and variety of materials studied require further research in order to understand how universal the correlations found are.

ACKNOWLEDGMENTS

This work was supported by funding from the Russian Fund for Fundamental Research (Grant No. 20-02-00314) and by State Assignment Grant No. AAAA-A21-121032400052-6.

[1] C. A. Angell, Science **267**, 1924 (1995).
[2] W. Kob and K. Binder, *Glassy Materials and Disordered Solids: An Introduction* (World Scientific, Singapore, 2011).
[3] W. Schirmacher, Phys. Status Solidi B **250**, 937 (2013).
[4] T. Nakayama, Rep. Prog. Phys. **65**, 1195 (2002).
[5] E. Duval, A. Boukenter, and T. Achibat, J. Phys. Cond. Matter **2**, 10227 (1990).
[6] E. Duval, L. Saviot, A. Mermet, L. David, S. Etienne, V. Bershtein, and A. J. Dianoux, J. Non-Cryst. Solids **307–310**, 103 (2002).
[7] A. Marruzzo, W. Schirmacher, A. Fratalocchi, and G. Ruocco, Sci. Rep. **3**, 1407 (2013).
[8] H. Mizuno, S. Mossa, and L. J. Barrat, Proc. Natl. Acad. Sci. USA **111**, 11949 (2014).
[9] S. Gelin, H. Tanaka, and A. Lemaitre, Nat. Mater. **15**, 1177 (2016).
[10] V. G. Karpov, M. I. Klinger, and F. N. Ignat'ev, Zh. Eksp. Teor. Fiz. **84**, 760 (1983) [Sov. Phys.-JETP **57**, 439 (1983)].
[11] U. Buchenau, Y. M. Galperin, V. L. Gurevich, and H. R. Schober, Phys. Rev. B **43**, 5039 (1991).
[12] V. L. Gurevich, D. A. Parshin, and H. R. Schober, Phys. Rev. B **67**, 094203 (2003).
[13] D. A. Parshin, H. R. Schober, and V. L. Gurevich, Phys. Rev. B **76**, 064206 (2007).
[14] M. Klinger, Phys. Reports **492**, 111 (2010).
[15] A. I. Chumakov, G. Monaco, A. Monaco, W. A. Crichton, A. Bosak, R. Rüffer, A. Meyer, F. Kargl, L. Comez, D. Fioretto *et al.*, Phys. Rev. Lett. **106**, 225501 (2011).
[16] T. S. Grigera, V. Martin-Mayor, G. Parisi, and P. Verrocchio, Nature (London) **422**, 289 (2003).
[17] S. Franz, G. Parisi, P. Urbani, and F. Zamponi, Proc. Natl. Acad. Sci. USA **112**, 14539 (2015).
[18] M. Baggioli and A. Zaccone, Phys. Rev. Lett. **122**, 145501 (2019).
[19] E. Lerner, G. Düring, and E. Bouchbinder, Phys. Rev. Lett. **117**, 035501 (2016).
[20] M. Wyart, S. R. Nagel, and T. A. Witten, Europhys. Lett. **72**, 486 (2005).
[21] V. Lubchenko and P. G. Wolynes, Proc. Natl. Acad. Sci. USA **100**, 1515 (2003).
[22] H. Tanaka, J. Phys. Soc. Jpn. **70**, 1178 (2001).
[23] W. Götze and M. R. Mayr, Phys. Rev. E **61**, 587 (2000).
[24] A. V. Granato, Physica B **219–220**, 270 (1996).
[25] V. G. Karpov, Phys. Rev. B **48**, 12539 (1993).
[26] P. G. DeBenedetti and F. H. Stillinger, Nature (London) **410**, 259 (2001).
[27] C. A. Angell, J. Non-Cryst. Solids **131–133**, 13 (1991).
[28] R. Böhmer, K. L. Ngai, C. A. Angell, and J. Plazek, J. Chem. Phys. **99**, 4201 (1993).
[29] D. Huang and G. B. McKenna, J. Chem. Phys. **114**, 5621 (2001).
[30] A. P. Sokolov, R. Calemczuk, B. Salce, A. Kisliuk, D. Quitmann, and E. Duval, Phys. Rev. Lett. **78**, 2405 (1997).
[31] V. N. Novikov and A. P. Sokolov, Nature (London) **431**, 961 (2004).
[32] T. Scopigno, G. Ruocco, F. Sette, and G. Monako, Science **302**, 849 (2003).
[33] V. N. Novikov, Y. Ding, and A. P. Sokolov, Phys. Rev. E. **71**, 061501 (2005).
[34] L. Battezzati, Mater. Trans. **46**, 2915 (2005).
[35] S. N. Yannopoulos and G. P. Johari, Nature (London) **442**, E7 (2006).
[36] V. N. Novikov and A. P. Sokolov, Phys. Rev. B **74**, 064203 (2006).
[37] G. Winterling, Phys. Rev. B **12**, 2432 (1975).
[38] R. J. Nemanich, Phys. Rev. B **16**, 1655 (1977).
[39] V. N. Novikov, E. Duval, A. Kisliuk, and A. P. Sokolov, J. Chem. Phys. **102**, 4691 (1995).
[40] O. Pilla, S. Caponi, A. Fontana, J. R. Gonçalves, M. Montagna, F. Rossi, G. Viliani, L. Angelani, G. Ruocco, G. Monaco *et al.*, J. Phys. Cond. Matt. **16**, 8519 (2004).
[41] J. Horbach, W. Kob, and K. Binder, Eur. Phys. J. B **19**, 531 (2001).
[42] W. Schirmacher, B. Schmid, C. Tomaras, G. Viliani, G. Baldi, G. Ruocco, and T. Scopigno, Phys. Status Solidi C **5**, 862 (2008).
[43] S. R. Elliott, Europhys. Lett. **19**, 201 (1992).
[44] P. H. Gaskell and D. J. Wallis, Phys. Rev. Lett. **76**, 66 (1996).
[45] P. S. Salmon, R. A. Martin, P. E. Mason, and G. J. Cuello, Nature (London) **435**, 75 (2005).
[46] A. P. Sokolov, A. Kisliuk, M. Soltwisch, and D. Quitmann, Phys. Rev. Lett. **69**, 1540 (1992).
[47] N. Als-Nielsen and D. McMorrow, *Elements of Modern X-Ray Physics* (Wiley, New York, 2011).
[48] S. Susman, D. L. Price, K. J. Volin, R. J. Dejus, and D. G. Montague, J. Non-Cryst. Solids **106**, 26 (1988).
[49] S. R. Elliott, J. Non-Cryst. Sol. **182**, 40 (1995).
[50] See Supplemental Material at http://link.aps.org/supplemental/10.1103/PhysRevE.106.024611 for the data supplementing Figs. 1–3 and additional details of the estimation of the self-energy function.
[51] J. C. Dyre, N. B. Olsen, and T. Christensen, Phys. Rev. B **53**, 2171 (1996).
[52] J. C. Dyre, Rev. Mod. Phys. **78**, 953 (2006).
[53] F. Fujara, B. Geil, H. Sillescu, and G. Fleischer, Z. Phys. B **88**, 195 (1992).
[54] I. Chang and H. J. Sillescu, Phys. Chem. B **101**, 8794 (1997).
[55] S. F. Swallen, K. Traynor, R. J. McMahon, M. D. Ediger, and T. E. Mates, J. Phys. Chem. B **113**, 4600 (2009).
[56] M. K. Mapes, S. F. Swallen, and M. D. Ediger, J. Phys. Chem. B **110**, 507 (2006).

[57] A. P. Sokolov and K. S. Schweizer, Phys. Rev. Lett. **102**, 248301 (2009).
[58] L.-M. Wang, C. A. Angell, and R. Richert, J. Chem. Phys. **125**, 074505 (2006).
[59] L.-M. Wang and J. C. Mauro, J. Chem. Phys. **134**, 044522 (2011).
[60] L.-M. Wang and R. Richert, Phys. Rev. B **76**, 064201 (2007).
[61] L.-M. Wang and R. Richert, Phys. Rev. Lett. **99**, 185701 (2007).
[62] A. F. Ioffe and A. R. Regel, Prog. Semicond. **4**, 237 (1960).
[63] H. Shintani and H. Tanaka, Nature Mater. **7**, 870 (2008).
[64] B. Rufflé, G. Guimbretière, E. Courtens, R. Vacher, and G. Monaco, Phys. Rev. Lett. **96**, 045502 (2006).
[65] W. Schirmacher, T. Scopigno, and G. Ruocco, J. Non-Cryst. Solids **407**, 133 (2015).
[66] Y. M. Beltukov, V. I. Kozub, and D. A. Parshin, Phys. Rev. B **87**, 134203 (2013).
[67] D. Quitmann, M. Soltwisch, and G. Ruocco, J. Non-Cryst. Solids **203**, 12 (1996).
[68] S. Kojima, V. N. Novikov, M. Kofu, and O. Yamamuro, Phys. Status Solidi B **257**, 2000073 (2020).
[69] G. Adam and J. H. Gibbs, J. Chem. Phys. **43**, 139 (1965).
[70] F. Puosi and D. Leporini, Eur. Phys. J. E **38**, 87 (2015).
[71] B. A. P. Betancourt, P. Z. Hanakata, F. W. Starr, and J. F. Douglas, Proc. Natl. Acad. Sci. USA **112**, 2966 (2015).
[72] M. Tsamados, A. Tanguy, C. Goldenberg, and J.-L. Barrat, Phys. Rev. E **80**, 026112 (2009).
[73] G. P. Shrivastav, P. Chaudhuri, and J. Horbach, Phys. Rev. E **94**, 042605 (2016).
[74] X. Wang, H. Zhang, and J. F. Douglas, J. Chem. Phys. **155**, 204504 (2021).
[75] Z. Pan, O. Benzine, S. Sawamura, R. Limbach, A. Koike, T. D. Bennett, G. Wilde, W. Schirmacher, and L. Wondraczek, Phys. Rev. B **104**, 134106 (2021).